Dependence of the Glass Transition Temperature of Polymer Films on Interfacial Energy and Thickness

David S. Fryer, Richard D. Peters, Eui Jun Kim, Jeanne E. Tomaszewski, Juan J. de Pablo, and Paul F. Nealey*

Department of Chemical Engineering and Center for Nanotechnology, University of Wisconsin, Madison, Wisconsin 53706

Chris C. White and Wen-li Wu

National Institute of Standards and Technology, Polymers Division, Gaithersburg, Maryland 20899-8541

ABSTRACT: The glass transition temperatures (T_g's) of ultrathin films (thickness 80−18 nm) of polystyrene (PS) and poly(methyl methacrylate) (PMMA) were measured on surfaces with interfacial energies (γ_{SL}) ranging from 0.50 to 6.48 mJ/m². The surfaces consisted of self-assembled films of octadecyltrichlorosilane (OTS) that were exposed to X-rays in the presence of air. Exposure to X-ray radiation systematically modified the OTS by incorporating oxygen-containing groups on the surface. The interfacial energy for PS and PMMA on the OTS surface was quantified as a function of X-ray dose using the Fowkes−van Oss−Chaudhury−Good model of surface tension. The T_g values of the films were characterized by three complementary techniques: local thermal analysis, ellipsometry, and X-ray reflectivity. Within the resolution of the techniques, the results were in agreement. At low values of γ_{SL}, the T_g values of PS and PMMA films were below the respective bulk values of the polymers. At high values of γ_{SL}, the T_g values of PS and PMMA films were higher than the bulk values and increased monotonically with increasing γ_{SL}. The deviation of the T_g values of the films compared to the bulk values increased with decreasing film thickness. For a specific film thickness of PS and PMMA, the difference between the T_g of the film and T_g of the bulk polymer ($\Delta T_g = T_g^{film} - T_g^{bulk}$) scaled linearly with γ_{SL} irrespective of the chemistry of the polymer.

Introduction

Knowledge of the properties of ultrathin polymer films is crucial for the design of many industrial products including paints, adhesives, and photoresists. Recent work has shown that the structure, wetting, and mobility of polymers in the form of ultrathin films differ greatly from the bulk.[1−5] For supported films, properties also depend on the substrate.[6] A well-documented property of thin polymer films that exhibits dimensional dependence is the glass transition temperature (T_g).[7−16] Recently, there has been great interest in quantifying the effect of the substrate on the T_g of ultrathin polymer films. Keddie and Jones performed the first study of the relative influence of two different substrates, gold and silicon oxide, on the T_g of ultrathin films of poly(methyl methacrylate) (PMMA).[13] By measuring thermal expansion of PMMA films with spectroscopic ellipsometry, they found that the T_g of PMMA decreased on gold substrates but increased on silicon oxide substrates. The authors attributed the difference in behavior to restricted mobility at the solid interface with silicon oxide due to hydrogen bonding. Forrest et al. compared the T_g's of freely standing polystyrene (PS) films to the T_g's of films supported or sandwiched between silicon oxide.[7] For similar film thickness, they observed significantly larger decreases in T_g compared to the bulk value for freely standing films than for supported films. The difference in T_g for supported films compared to sandwiched films (supported films capped with silicon oxide layers deposited by evaporation), however, was small.

On the basis of these observations, the authors concluded that the nature of the interaction of the polymer with the substrate must be the dominant factor in determining dimension-dependent glass transition temperatures of supported films.

In the course of developing local thermal analysis as a technique to determine the T_g of polymer thin films, we measured the T_g of PS and PMMA supported on substrates of silicon oxide and on substrates of silicon oxide treated with hexamethyldisilizane (HMDS).[9] The T_g of PMMA films increased relative to the bulk value on silicon oxide (a polar surface) and decreased relative to the bulk value on silicon oxide treated with HMDS (a nonpolar surface) with decreasing film thickness. The T_g of PS decreased relative to the bulk value for ultrathin films on both types of substrates with decreasing film thickness.

Several authors have proposed models of T_g behavior in which the polymer films are considered to consist of three layers; the dynamics of the material and thus the glass transition temperature of each layer are postulated to be different.[8,10,17] Near the free surface the chain mobility is considered to be greater than in the bulk polymer. In the center of the film, the chain mobility is considered equivalent to the bulk polymer. And at the solid interface, mobility is restricted relative to bulk polymer. Models based on this approach fit the experimental data quite well. Investigations employing molecular simulation appear to support the layer model. Bashnagel and Binder performed dynamic Monte Carlo simulations of a supercooled polymer melt confined between two neutral hard interfaces.[18] Their results

* Corresponding author: nealey@engr.wisc.edu.

indicated that the presence of an interface causes an increase in the local density that extends into the bulk. They concluded that a competition between packing constraints in the bulk and the loss of configurational entropy at the solid interface led to greater monomer and end-monomer density at the solid interface. Torres et al. performed molecular dynamics simulations of polymer films supported on a substrate in which they included a variable attractive intermolecular potential between the polymer and the substrate.[19] The T_g values of ultrathin films (<60 nm thick) increased as the intermolecular potential between the polymer chains and the substrate increased. The simulations clearly revealed reduced mobility of the polymer chains as a result of attractive forces at the interface.

The previous experimental and theoretical work raises the question of how to parametrize the interaction between the polymer and substrate in order to predict the behavior of T_g of supported films as a function of film thickness. In this paper we report experimental results quantifying the effect of interfacial energy between the polymer and the substrate on the dimension dependent glass transition temperatures of thin polymer films. The substrates consisted of thermally stable self-assembled (SA) films of octadecyltrichlorosilane (OTS) on silicon wafers. The interfacial energy between the substrates and PS and PMMA was tuned by exposing the OTS to different doses of X-rays in the presence of air.[20] Exposure to X-ray radiation systematically modified the OTS by incorporating oxygen-containing groups on the surface, and the interfacial energy for both polymers increased with increasing exposure dose. We found that (1) T_g's were decreased from the bulk values at low values of the interfacial energy (γ_{SL}), (2) T_g's were increased from the bulk values at high values of γ_{SL}, (3) the deviation in the T_g from the bulk value increased with decreasing thickness of the film, and (4) the deviation in T_g from the bulk value was linearly dependent on the interfacial energy independent of the chemistry of the polymer film for a constant film thickness. The T_g's of the films were determined using three complementary techniques: local thermal analysis, ellipsometry, and X-ray reflectivity (XRR). Using ellipsometry and X-ray reflectivity, T_g is determined by measuring changes in the thermal expansion of the film. Ellipsometry is perhaps the most established technique to determine the T_g of thin polymer films, and X-ray reflectivity provides the most accurate data to quantify the coefficients of thermal expansion (CTE) in the glassy and rubbery regimes. Using local thermal analysis, on the other hand, T_g is determined by measuring changes in the heat capacity and thermal conductivity of the film and the area of contact between the probe and the polymer surface. The fact that all three techniques yield similar results establishes credibility for all of the techniques and precludes any possibility that the phenomena described here are experimental artifacts.

Experimental Procedure

Materials. Polished test grade silicon ⟨100⟩ wafers were purchased from Tygh Silicon.[21] Octadecyltrichlorosilane (CH3-(CH2)17SiCl3, 95%) was purchased from Gelest and was used as received. Polystyrene (M_w = 382.1 kg/mol, polydispersity (PD) = 1.16) was purchased from Aldrich. Poly(methyl methacrylate) (M_w = 100.3 kg/mol, PD = 1.04 and M_w = 520 kg/mol, PD = 1.02) was purchased from Polysciences Inc. Higher molecular weight polystyrene (M_w = 560 kg/mol, PD = 1.02)

was also purchased from Polysciences Inc. Toluene (99.8%, anhydrous), chloroform (99+%, anhydrous), glycerol (99+%), and diiodomethane (99%) were purchased from Aldrich and were used without further purification (the percentages are by mass and are obtained from the manufacturer). Ethanol (dehydrated, 200 proof) was purchased from Aaper Alcohol and Chemical Co. and was used as received.

Deposition of Self-Assembled Films of OTS. For thermal probe and ellipsometry analysis silicon wafers were cleaved into pieces approximately 1 cm × 2 cm and were cleaned by immersion in a piranha solution (4/1 (m/m) of 98% H2SO4/30% H2O2; *caution: piranha solution reacts violently with organic compounds and should not be stored in closed containers*) at 100 °C for 30 min. The silicon substrates were immediately rinsed with deionized water (resistivity ≥ 18 MΩ·cm) several times and were blown dry with nitrogen. The clean substrates were immersed in a 0.06% (m/m) solution of OTS in toluene in a glovebox with a nitrogen atmosphere. The immersion time (~24 h) was optimized from kinetic studies of contact angle and thickness for formation of films with thickness of 2.6 nm (the calculated thickness of fully extended high-density chains) and with maximized contact angles with water (~110°). After the substrates were removed from the silane solution, they were rinsed with chloroform for approximately 30 s, and excess chloroform was allowed to evaporate. The SA films (CH3(CH2)17SiO−/SiOx) were baked at 120 °C for 5 min and then were removed from the glovebox. The SA films were rinsed with absolute ethanol and were dried under a stream of nitrogen.

SA films were also deposited on 0.635 cm thick, 10.16 cm diameter silicon wafers after cleaning for the X-ray reflectivity experiments. It was difficult to deposit homogeneous SA films on these large substrates, and thus the surfaces for the X-ray reflectivity experiments were not as well characterized as the surfaces for the thermal probe and ellipsometry experiments.

Exposure of Self-Assembled Films to X-rays. The SA films were irradiated with soft X-rays in the ES-1 beamline at the Center for Nanotechnology (CNT). CNT facilities are located at the Synchrotron Radiation Center at the University of Wisconsin. The wavelength (λ) of the broad-band radiation was centered at 1.1 nm with $\lambda/\Delta\lambda \approx 3$. The intensity of the incident radiation was 17−38 mW/cm² and varied with the synchrotron ring current. Samples were irradiated at an incident angle of 90°. The exposures were carried out in a chamber with a pressure of 133 Pa of ambient air. The intensity of the X-ray beam was attenuated when passing through the atmosphere of the chamber. The reported doses from 0 to 2000 mJ/cm² refer to the dose that is delivered to the chamber. The effective dose that reached the surface of the monolayers was approximately 93 ± 2% (the uncertainty value shown is our estimate of the precision of the experimental design) of the reported dose. Advancing contact angles of water, glycerol, and diiodomethane were measured using a Future Digital Scientific model OCA15 video contact angle system within 2−3 h after irradiation. Polymer thin films also were deposited on the exposed SA films within 2−3 h after irradiation.

Sample Preparation. For the samples measured with local thermal analysis and ellipsometry, the PS and PMMA solutions were directly spin-cast onto the wafers treated with OTS. The polymers (PS and PMMA) were dissolved in toluene. The solution concentrations varied from 0.25 to 2% by mass. The polymer solutions were filtered (1 μm Teflon filters) prior to spin-casting. A Headway Research spinner was used to spin-cast PS and PMMA on the substrates. The spinner was operated at 2000 rad/s for 45 s for each application. The polymer-coated substrates were annealed at 135 °C (PS) or 145 °C (PMMA) for 12 h in a VWR Scientific vacuum oven. After 12 h, samples were allowed to cool to room temperature at ~1 °C /min.

For X-ray reflectivity analysis, polystyrene was dissolved in toluene with a concentration of 1.3% by mass. These solutions were allowed to stand for 24 h before the films were spin-cast. A Headway spin coater was used to spin-cast the ultrathin polymer films. The thickness of the film was 62 ± 2

Table 1. Measured Contact Angles of Water, Glycerol, and Diiodomethane on a Self-Assembled Film of OTS Exposed to X-rays in Air and the Calculated Interfacial Energies from the FOCG Model of Surface Tension[a]

X-ray dose (mJ/cm²)	advancing contact angle (deg)			interfacial energy (mJ/m²)	
	water	glycerol	diiodomethane	γ_{SL} (PS)	γ_{SL} (PMMA)
500	93.5 ± 0.3	86.7 ± 0.3	64.6 ± 1.3	0.8 ± 0.1	1.3 ± 0.2
1250	63.1 ± 0.9	63.5 ± 0.4	45.8 ± 0.6	1.7 ± 0.2	0.5 ± 0.1
2000	37.3 ± 0.4	45.0 ± 0.3	37.1 ± 1.5	6.5 ± 0.2	3.3 ± 0.2

[a] The uncertainty values in the reported contact angles are the relative standard deviation of three independent measurements. The uncertainty values in the reported interfacial energies are due to the error in the contact angles.

nm for all five wafers. Each film was spin-cast onto a clean silicon wafer, floated off the surface of the silicon wafer onto 18 MΩ·cm water, and placed on the surface of a wafer treated with SA films of OTS. The PMMA films were spin-cast from a solution of PMMA dissolved in *o*-xylene at a concentration of 1.3% by mass. This resulted in slightly thicker PMMA films with all five films having a thickness of 80 ± 3 nm. PMMA films were also applied to the surface of a wafer treated with SA layers of OTS by floating from a clean silicon wafer. Both the PMMA and PS samples were annealed under high vacuum at 150 ± 1 °C for 12 h to remove any residual solvent or water. Serial dilution and spin-casting of the polymer solution was employed to prepare the different thickness samples. The resulting thicknesses ranged from 181 to 29 nm.

Local Thermal Analysis. Resistive thermal probes connected to a thermal control unit were mounted in a Voyager scanning probe microscope equipped with an Explorer scanning head (Thermomicroscopes) to measure the glass transition temperature for polymer films supported on X-ray-exposed OTS. Using a technique called local thermal analysis, the thermal probe was placed in contact with the sample surface and heated (contact area with the surface is approximately 0.3 μm^2). The thermal control unit is a device that sets the resistance of the probe by changing the current through it with 0.05 Ω precision resistors connected to a Wheatstone bridge.[22] Based on the ratio of the fixed resistors in the Wheatstone bridge, the resistance of the probe was set within ±0.01 Ω. The probe was a platinum/10% rhodium thermistor material that has a known dependence of temperature on resistance. The temperature of the probe was calibrated at one value of resistance (using the melt transition of a long chain alkane, hexatriacontane), thus defining the entire temperature vs resistance behavior of the probe. During measurement of a polymer film, the temperature of the probe was ramped from room temperature to temperatures as high as 200 °C by increments of 2.5 °C at 30 s intervals. At each temperature set point, the power provided to the thermal probe to maintain a constant temperature was recorded. Over a range of temperatures including the T_g, the power supplied to the probe increased as the set point temperature of the probe increased. The increase in power associated with the T_g event was best observed by plotting the derivative of power supplied to the probe as a function of temperature. The onset of the increase in the derivative signal as the set point of the temperature of the probe was ramped upward was identified as the T_g of the polymer film. A more detailed description of the experiment and the analysis can be found in ref 9. The scans shown in this report are chosen as a representative of one of three or more scans taken on each film. At least three scans with comparable values of T_g (within 3 °C) were gathered for each sample.

Ellipsometry. The thicknesses of the polymer films as a function of temperature were determined using an Auto EL nulling ellipsometer (Rudolph) at three wavelengths: 632.8, 546, and 405 nm. The polymer film samples were placed on a hot plate (Reichert-Jung) mounted on the optical stage of the ellipsometer. The angle of incidence of the beam was 70° to the sample. The resolution of the instrument was ±0.04° in Δ and Ψ. For a given sample, the film thickness was measured at room temperature and then over a range of temperatures up to 140−160 °C. The film thickness was determined at temperature increments that varied between 2.6 and 10.5 °C, with an average increment of 5.3 °C. Each value of the film

thickness was determined during the heating process by holding the hot plate at the desired temperature for approximately 10 min. The values of film thickness were then determined with a single-layer model (polymer film on a silicon substrate) using FilmEllipse software (version 1.1, Scientific Company, Intl.) and all three values of Δ and Ψ. The accuracy of this model was confirmed by checking room temperature thickness values with both scanning force microscopy measurements (Thermomicroscopes) and profilometry measurements (Alpha Step). In all cases, the thickness values determined from a single-layer model were within 5% of the values determined from either of the contact methods. The values of T_g and CTE were determined from a linear least-squares fit to the data. Results reported herein had an average R^2 value of 0.98; the lowest R^2 fit was 0.96. T_g was identified as the temperature at which the slope of the line relating thickness and temperature (i.e., the CTE) changed value.

X-ray Reflectivity. The thickness, roughness of both the top and bottom interfaces, and electron density were determined by X-ray reflectivity on a Scintag (XDS 2000) for the polymer films. This technique involves experimentally determining the intensity of the reflected X-rays as a function of the scattering vector, $q = 4\pi/\lambda(\sin\theta)$, where λ is the wavelength and θ is the specular reflection angle, and then determining the properties by fitting to a model electron density profile. The model profile prediction is then compared to the experimental data of the specular reflected intensity vs q. The model is then modified until a satisfactory match of the experimental data and model prediction is achieved. The experimental thickness, roughness, and electron density of the ultrathin polymer films are identical to the model layer. The details of this technique are presented elsewhere.[23] The thickness was determined with a standard uncertainty of ±0.2 nm. This estimate of the uncertainty in the thickness is achieved by making small perturbations in the model predictions to generate a 10% increase in the χ^2 test of the fit of the model predictions to the experimental data. The X-ray intensity vs q and subsequent model fitting were determined for each polymer film, on a silicon substrate, for a temperature range of 20−170 °C. Each sample was placed on the sample stage and enclosed inside a vacuum chamber. Each film on silicon substrates was then held under vacuum for 12 h at 170 °C. Following the annealing, the X-ray intensity vs q was determined. The temperature set point was then reduced by 10 °C, following 45 min to establish thermal equilibrium. The X-ray intensity vs q was again determined. This procedure was repeated for the temperature range of 150 °C down to 20 °C. For one set of PS samples, additional data were collected using the same procedure as outlined above but starting at 20 °C and increasing to 170 °C in 10 °C increments.

Results and Discussion

Characterization of Polymer−Substrate Interaction. The contact angles of water, gycerol, and diiodomethane on SA films of OTS exposed to different doses of radiation are listed in Table 1. Hydroxyl (C−OH) and aldehyde (C=OH) functional groups were incorporated onto the surface of OTS as the films are exposed to X-rays in the presence of oxygen.[24] The contact angles of all three liquids measured (water, glycerol, and diiodomethane) decreased with dose as the concentration of oxidized groups on the surface of the

OTS increased.[20] The contact angle values were used as input into the Fowkes−van Oss−Chaudry−Good (FOCG) model of surface tension to calculate surface tensions of exposed SA films and interfacial energies (γ_{SL}) between the exposed OTS and homopolymers of PS or PMMA. The FOCG model predicts the interfacial energy based on the combination of attractive van der Waals forces (or dispersive interactions) and Lewis acid−base polar interactions (or hydrogen bonding). In this model, the surface tension is comprised of three parameters and is given by

$$\gamma^{total} = \gamma^{LW} + 2\sqrt{\gamma^{+}\gamma^{-}} \qquad (1)$$

where γ^{LW} is the Lifshitz−van der Waals (or dispersive) component, γ^{+} is the electron-acceptor component, and γ^{-} is the electron-donor component. The three solid surface tension parameters (γ_{S}^{LW}, γ_{S}^{+}, and γ_{S}^{-}) are related to the contact angle of a liquid on a surface through the modified Young−Dupré equation:

$$(1 + \cos\theta)\gamma_{L} = 2(\sqrt{\gamma_{S}^{LW}\gamma_{L}^{LW}} + \sqrt{\gamma_{S}^{+}\gamma_{L}^{-}} + \sqrt{\gamma_{S}^{-}\gamma_{L}^{+}}) \qquad (2)$$

where the subscript L refers to liquid surface tension parameters and γ_{L} is the total liquid surface tension against air. To find the three parameters for the solid surface (γ_{S}^{LW}, γ_{S}^{+}, and γ_{S}^{-}), three independent equations are obtained by measuring the contact angles of three liquids (two of which must be polar) with known values of γ_{L}^{LW}, γ_{L}^{+}, and γ_{L}^{-} on the solid surface. The surface tension parameters of the three test liquids we used in this study were taken from the literature.[25]

The interfacial energies of PS and PMMA homopolymers on each type of surface were determined using the FOCG model. Using the Good−Girifalco−Fowkes combining rule[26] and expressions for the Lewis acid−base interactions across the interface,[27] γ_{SL} between the solid and a liquid was calculated using

$$\gamma_{SL} = (\sqrt{\gamma_{S}^{LW}} - \sqrt{\gamma_{L}^{LW}})^2 + 2(\sqrt{\gamma_{S}^{+}\gamma_{S}^{-}} + \sqrt{\gamma_{L}^{+}\gamma_{L}^{-}} - \sqrt{\gamma_{S}^{+}\gamma_{L}^{-}} - \sqrt{\gamma_{S}^{-}\gamma_{L}^{+}}) \qquad (3)$$

The surface tension parameters of PS and PMMA were previously determined.[20] The calculated γ_{SL} of PS and PMMA on the exposed SA films (listed in Table 1) are given in Table 1. The calculated values of the γ_{SL} shown in Table 1 increased monotonically with increasing dose for PS. For PMMA, γ_{SL} decreased initially then increased with increasing dose.

Since the contact angles of the test liquids were measured at room temperature, the values for γ_{SL} in Table 1 correspond to a temperature of 25 °C. Ideally, γ_{SL} should be determined at the temperature of interest, i.e., temperatures near the T_{g}'s of the polymer films. We were unable to measure γ_{SL} at elevated temperatures due to volatility of the test liquids and increased solubility or increased kinetics of dissolution of PS and PMMA by the test liquids. Conclusions can be drawn regarding the generalized behavior of T_{g} as a function of γ_{SL}, however, using the room temperature values based on the well-behaved way in which γ_{SL} varies with temperature. Wu measured interfacial energies between a number of polymers at temperatures between 20 and 180 °C.[28] For PS and PMMA in contact with poly-(ethylene) (PE), a model of PS and PMMA in contact
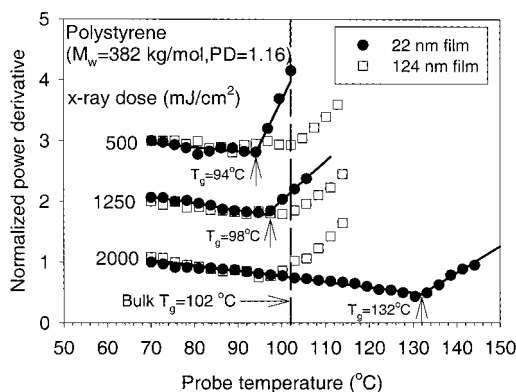
Figure 1. Plot of the power derivative, for 22 and 124 nm thick PS films on OTS exposed to X-ray radiation in air, as a function of temperature. The power derivative was normalized to the value at the lowest probe temperature (70 °C). Scans at different exposure doses are shifted for clarity.

with OTS exposed to low doses of X-rays, $\Delta\gamma_{PS-PE}/\Delta T = -0.02$ mJ/(m² K) and $\Delta\gamma_{PMMA-PE}/\Delta T = -0.018$ mJ/(m² K) for 20 °C < T < 180 °C. $\Delta\gamma_{SL}/\Delta T$ for PS or PMMA in contact with OTS are thus expected to be nearly equal in value over the temperature range of interest. We do not, however, expect the magnitude of $\Delta\gamma_{SL}/\Delta T$ for PS or PMMA in contact with OTS exposed to low doses of X-rays to be as large as the magnitude of $\Delta\gamma_{SL}/\Delta T$ for PS and PMMA in contact with PE; otherwise, γ_{SL} would be calculated to be negative at temperatures near 100 °C. An analogy for $\Delta\gamma_{SL}/\Delta T$ for PS and PMMA in contact with OTS exposed to high doses of X-rays in Wu's measurements of polymer/polymer interfacial energies is not readily apparent. In our data, PS and PMMA, a nonpolar and a polar polymer, respectively, are in contact with OTS exposed to high doses of X-rays, a polar surface. In Wu's data, PS and poly(*n*-butyl methacrylate) (PnBMA) in contact with PMMA may be considered as a nonpolar and polar polymer, respectively, in contact with a relatively polar surface, and $\Delta\gamma_{PS-PMMA}/\Delta T = -0.0125$ mJ/(m² K) is identical to $\Delta\gamma_{PnBMA-PMMA}/\Delta T = -0.0125$ mJ/(m² K) for 20 °C < T < 180 °C. On the basis of Wu's data, we conclude that (1) the absolute values of γ_{SL} at elevated temperatures will be approximately 1−2 mJ/m² less than the room temperature values listed in Table 1 and (2) trends (slopes) reported in T_{g} as a function of the room temperature values of interfacial energy will be at least qualitatively if not semiquantitatively correct. Further evidence to support these conclusions can be drawn from our experiments investigating the wetting behavior of diblock copolymer films on OTS exposed to increasing doses of X-rays.[20] We interpreted the observation of symmetric, neutral, and asymmetric wetting behavior of polymer films annealed at 180 °C in terms of room temperature values of γ_{SL} (determined using the FOCG model) for PS and PMMA in contact with exposed OTS. The dose at which we observed neutral wetting of the block copolymer at 180 °C corresponded to the dose at which the room temperature values of γ_{SL} for PS and PMMA in contact with the exposed OTS were equal.

**Determination of T_{g} of PS and PMMA Films Using Local Thermal Analysis.** A plot of the normalized derivative of power, as a function of probe temperature, for PS films on substrates of OTS exposed with X-ray radiation is shown in Figure 1. The derivative of the power was normalized to the value at the lowest probe temperature shown on the plot (70 °C). The
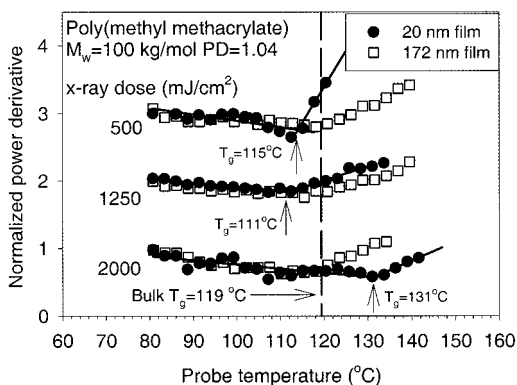
Figure 2. Plot of the power derivative, for 20 and 172 nm thick PMMA films on OTS exposed to X-ray radiation in air, as a function of temperature. The power derivative was normalized to the value at the lowest probe temperature (80 °C). Scans at different exposure doses are shifted for clarity.

Figure 3. Plot of the difference in the glass transition temperature, between the film and the bulk, as a function of interfacial energy for PS and PMMA films of three different thicknesses. The results were extracted from thermal probe measurements. The dashed line is a linear regression of the data for both 22 nm PS films and 20 nm PMMA films.

thermal scan for each exposure dose is offset for clarity. The behavior of the derivative of the power signal was similar for all scans, decreasing with increasing temperature at probe temperatures well below the bulk T_g and then increasing at higher probe temperatures. Note that the power derivative is always positive, i.e., the heat flux from the probe to the polymer film is always increasing with temperature. This behavior is primarily due to the decrease in the thermal conductivity of the silicon substrate with increasing temperature. When a thermal scan is performed on bare silicon, without a polymer film present, a more pronounced trend to lower positive derivative values with increasing temperature is observed. The decrease in the magnitude of the derivative with increasing temperature varies to some extent with film thickness and film material. Results from two thermal scans, one for a 22 nm film and one for a 124 nm film, are plotted together for each exposure dose. Thick film results are plotted for comparison to show the temperature resolution of the technique (~2.5 °C) and the reproducibility of the probe temperature where the increase in the derivative signal occurred over a range of X-ray exposure doses. The average T_g for thick films on all surfaces was 102 ± 3 °C. For 22 nm films T_g occurred at a probe temperature that varied with exposure dose. For exposure doses of 500 and 1250 mJ/cm^2, the T_g was 8 and 4 °C below the bulk glass transition temperature, respectively. For an exposure dose of 2000 mJ/cm^2, the T_g was 30 °C above the bulk glass transition temperature.

Figure 2 shows a plot of the normalized derivative of power, as a function of probe temperature, for PMMA films on substrates of OTS exposed with X-ray radiation. The format for the data is the same as in the previous plot; the derivative of the power was normalized to the value at the lowest probe temperature (80 °C), and scans for each exposure dose were offset for clarity. Two scans at each exposure dose correspond to data for a 20 and 172 nm film. For 172 nm films, the increase in the derivative of the power occurred at a probe temperature equal to the bulk glass transition temperature (T_g = 119 °C). For 20 nm films, the T_g occurred at a probe temperature that varied with exposure dose. The probe temperature at the onset of the change in derivative signal did not increase monotonically with exposure for PMMA. The T_g first decreased and then increased with exposure dose, as did γ_{SL}. Note that, upon entering the melt temperature regime, increases in heat capacity and
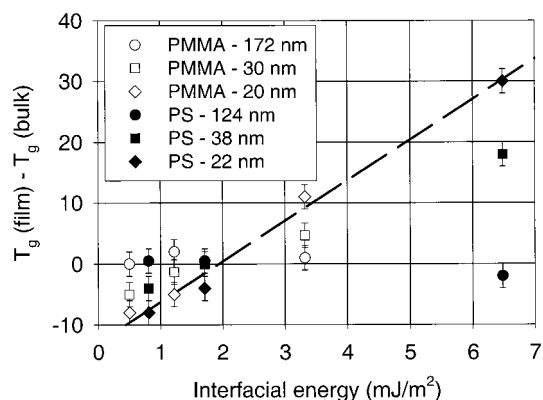
thermal conductivity and contact area between the probe and the film contribute to the increase in slope of the power derivative. Based on the measurements in Figures 1 and 2, in films supported on low-dose surfaces, the increase in slope at the T_g from these combined effects is larger than the increase in slope at the T_g for high-dose surfaces (PS melt slopes: 0.146 mW/°C^2 for 500 mJ/cm^2, 0.069 mW/°C^2 for 1250 mJ/cm^2, and 0.059 mW/°C^2 for 2000 mJ/cm^2; PMMA melt slopes: 0.106 mW/°C^2 for 500 mJ/cm^2, 0.021 mW/°C^2 for 1250 mJ/cm^2, and 0.028 mW/°C^2 for 2000 mJ/cm^2). The origin of this difference in behavior is unknown.

In Figure 3, the difference in the value of T_g measured by local thermal analysis and the bulk T_g is plotted as a function of interfacial energy for three values of the film thickness for PS and PMMA. For 124 nm thick PS films and 172 nm thick PMMA films, there was no apparent dependence of the T_g on the interfacial energy. However, for the films measured that were less than 40 nm thick in both polymers, there was a strong dependence on the interfacial energy. For higher energy surfaces with γ_{SL} greater than approximately 2 mJ/m^2, the measured T_g was higher than the bulk glass transition temperature. For γ_{SL} below 2 mJ/m^2, the measured T_g was less than the bulk value. The dependence of T_g on interfacial energy is greatest for the 20 and 22 nm films. Since the thinnest PS and PMMA films are of similar thickness (~20 nm), a fit to both sets of data was performed. A linear regression provides an excellent fit (R^2 = 0.989) of the data where the slope of the linear fit is 7 °C/(mJ/m^2).

Our previous measurements of the T_g of PS and PMMA on silicon wafers treated with HMDS are qualitatively consistent with these results.[9] The interfacial energy for these polymers in contact with HMDS surface prepared in a similar way to our previous experiments, calculated from the same model, is less than 2 mJ/m^2 (θ_w = 83.1°, θ_g = 85.2°, θ_d = 68.0°), and the measured glass transition temperature is less than the bulk value for ultrathin films of PS (γ_{SL} = 1.9 ± 0.5 mJ/m^2) and PMMA (γ_{SL} = 1.6 ± 0.2 mJ/m^2). The effect of interfacial energy on the T_g of ultrathin films has not been generalized to other types of substrates on which the T_g of PS and PMMA has been determined: silicon oxide, silicon hydride, and gold. We have not determined γ_{SL} for these substrates, and these substrates are fundamentally different than those included in this

study. They represent hard surfaces (the modulus of silicon oxide is ~70 GPa), whereas the SA films are soft surfaces (the modulus of the SA films is ~13 GPa[30]).

If the segmental mobility of polymer in a region near the substrate depends on interfacial energy, then the results presented above are consistent with layer models of the T_g of ultrathin polymer films. The layer of polymer near the free surface always increases the overall mobility, a middle layer behaves like bulk polymer, and the solid interface can either decrease, increase, or render the mobility of the polymer unchanged compared to the bulk. Interpretation of our experimental results in terms of the layer model is as follows: low interfacial energy must result in increased segmental mobility and high interfacial energy must result in decreased segmental mobility near the substrate compared to the bulk. A weighted average of the mobility of the layers according to the relative dimensions of the layers determines the T_g of the entire film.

Insight concerning the decrease in segmental mobility of polymer chains with increasing interfacial energy can be gained from the results of molecular dynamics simulations. Torres et al. represented polymer molecules in their simulations using square-well interaction sites interconnected by fully flexible strings.[19] For supported films, an attractive wall represented the substrate. If the attractive potential, ϵ, between the interaction sites of the polymer chains and the wall was the same ($\epsilon = 1$) as the attractive potential between polymer–polymer sites, the wall was considered to be "weakly" attractive, and T_g decreased compared to the bulk polymer but did not decrease as much as simulated free-standing films with the same thickness. If ϵ between the interaction sites of the polymer chains and the wall was doubled ($\epsilon = 2$), then the wall was considered to be "strongly" attractive and T_g increased compared to the bulk polymer. Analysis of total mean displacement of segments as a function of temperature and position in the film showed that the mobility of the polymer near the substrate decreased for increasing ϵ. The exact relationship between ϵ and γ_{SL} requires integration of differences in components of the pressure tensor over the thickness of the film.[31] Since these calculations are unavailable, we resort to scaling arguments that predict γ_{SL} increases with the square root of ϵ. From experiments, layer models, and molecular simulation results, it is clear that the mobility of polymer segments near the substrate decreases as the interfacial energy increases and that the nature of the substrate–polymer interface dominates the T_g behavior of ultrathin films.

Beyond discussion of the observed phenomena regarding the T_g of free-standing and supported films presented in this paper and elsewhere, however, there is still little understanding of why surface and interfacial effects that act over a length scale considerably shorter than the thickness of the films affect or propagate through out the entire film and have such a profound influence on thermophysical properties. According to theoretical arguments, the length scale over which cooperative chain motion in the bulk exists at T_g is of order 1–2 nm.[32] Reconciliation between the length scale over which deviations in the T_g in thin films are observed (up to ~50 nm) and the apparent length scale of the T_g event (~2 nm) remains elusive.

To provide a direct comparison between different experimental techniques and to further explore the relationship between T_g and interfacial energy, we
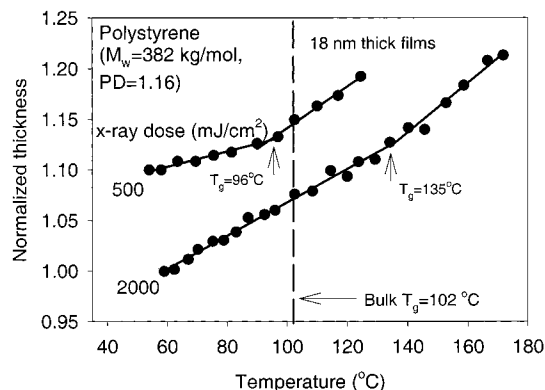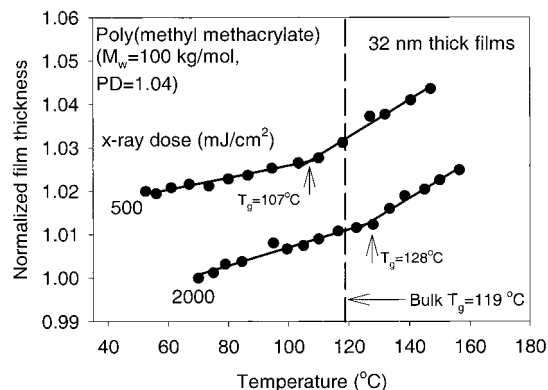

Figure 4. Plot of the normalized film thickness, for 18 nm PS films on OTS exposed with X-ray radiation, as a function of temperature measured with ellipsometry. The film thickness was normalized to the value at the lowest film thickness. Scans at different exposure doses are shifted for clarity.

measured the thermal expansion of ultrathin PS and PMMA films on the same surfaces with ellipsometry and X-ray reflectivity. The results using these methods confirm the observations from local thermal analysis; the measured T_g in ultrathin polymer films scales linearly with the interfacial energy of the substrate.

Determination of T_g and CTE of PS and PMMA Films Using Ellipsometry. A plot of the normalized thickness of 18 nm PS films supported on OTS as a function of temperature for two different doses of X-ray radiation, 500 and 2000 mJ/cm², is shown in Figure 4. The two sets of data were normalized to the thickness at approximately 56 °C (500 mJ/cm² result) and 60 °C (2000 mJ/cm² result) and offset for clarity. Similar to the behavior reported in previous work, the slope of the thermal expansion of the film increased at the glass transition temperature. The measured CTE of the glass ($\alpha_{glass} = 4.2 \times 10^{-5}$ K^{-1} for 500 mJ/cm² and $\alpha_{glass} = 9.2 \times 10^{-5}$ K^{-1} for 2000 mJ/cm²) and the melt ($\alpha_{melt} = 1.1 \times 10^{-4}$ K^{-1} for 500 mJ/cm² and $\alpha_{melt} = 1.4 \times 10^{-4}$ K^{-1} for 2000 mJ/cm²) were influenced by the substrate[29] and are approximately a factor of 2 less than bulk values. The disparity between bulk and film CTE values measured with ellipsometry can be attributed to the temperature dependence of the optical properties of the oxide layer[29] that supports both the OTS and polymer films in the experiment; while the film is expanding, there is a contributing effect of the substrate to the measured value of thickness. However, the ratio of the glass to melt CTE's is consistent with bulk behavior for the 500 mJ/cm² data ($\alpha_{melt}/\alpha_{glass} = 2.6$, $\alpha_{melt}/\alpha_{glass}$ is approximately 2–3 for bulk PS) and only slightly below it for the 2000 mJ/cm² data ($\alpha_{melt}/\alpha_{glass} = 1.5$). The increase in slope of thermal expansion between the glass and melt regime is large and allows clear identification of the transition. Based on a best fit of two straight lines to the data at temperatures above and below the change in thermal expansion of the film, the glass transition temperatures were 96 and 135 °C for the 500 and 2000 mJ/cm² films, respectively. These results were in good agreement with thermal probe measurements of the same films ($T_g = 94$ and 132 °C for approximately the same film thickness measured with local thermal analysis).

A plot of the normalized thickness of 32 nm poly-(methyl methacrylate) films supported on a SA layer surface as a function of temperature for two different doses of X-ray radiation, 500 and 2000 mJ/cm², is shown

Figure 5. Plot of the normalized film thickness, for 32 nm PMMA films on OTS exposed with X-ray radiation, as a function of temperature measured with ellipsometry. The film thickness was normalized to the value at the lowest film thickness. Scans at different exposure doses are shifted for clarity.

in Figure 5. The two sets of data were normalized to the thickness at approximately 56 °C (500 mJ/cm² results) and 70 °C (2000 mJ/cm² results) and offset for clarity. Again, the measured coefficients of thermal expansion of the glass ($\alpha_{glass} = 6.5 \times 10^{-6}$ K^{-1} for 500 mJ/cm² and $\alpha_{glass} = 4.3 \times 10^{-6}$ K^{-1} for 2000 mJ/cm²) and the melt ($\alpha_{melt} = 1.3 \times 10^{-5}$ K^{-1} for 500 mJ/cm² and $\alpha_{melt} = 1.3 \times 10^{-5}$ K^{-1} for 2000 mJ/cm²) were influenced by the substrate.[29] The increase in slope of thermal expansion between the glass and melt regimes is large (α increases by a factor of 2.0 and 3.0 for the 500 and 2000 mJ/cm² data sets, respectively) and allows clear identification of the transition. Based on a best fit of two straight lines to the data at temperatures above and below the change in slope, the glass transition temperatures were 107 and 128 °C for the 500 and 2000 mJ/cm² films, respectively. The values of T_g measured with ellipsometry were within 8 °C of the local thermal analysis result for somewhat thinner films that were 20 nm thick.

Determination of T_g and CTE of PS and PMMA Films Using X-ray Reflectivity. Plots of the increase in polymer thickness for 62 nm PS films and 80 nm PMMA films with temperature for five different doses of X-ray radiation on SA layers of OTS measured with XRR are shown in parts a and b of Figure 6, respectively. The solid circles are the data collected on decreasing temperature increments (170−20 °C), and the open circles are the data collected on increasing temperature increments (20−170 °C). The solid lines represent the predicted value of film expansion with temperature assuming bulk properties (coefficient of thermal expansion, Poisson ratio, and glass transition temperature). The film thickness values (predicted and actual) are offset in the plots for clarity. For the PS films studied, there was no observed dependence of thickness on direction of the temperature ramp. Independent of whether the film was heated or cooled, approximately the same value of film thickness was measured. In addition, there was no observed dependence of the CTE on the substrate studied. Above the glass transition temperature, the CTE of all the films was equivalent to the bulk CTE of rubbery polystyrene. However, there was a significant departure from predicted bulk temperature at which the glass transition occurred depending on the X-ray exposure dose to the OTS. For both polymers, the increase in exposure dose to the OTS
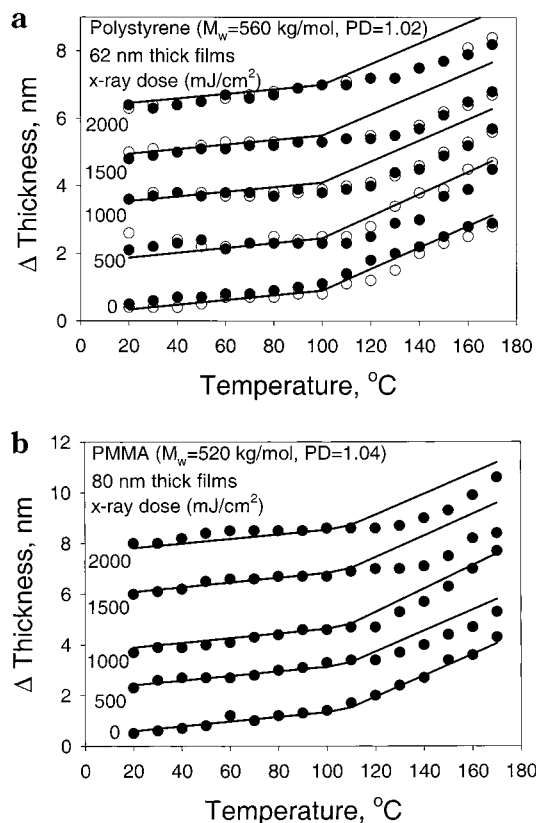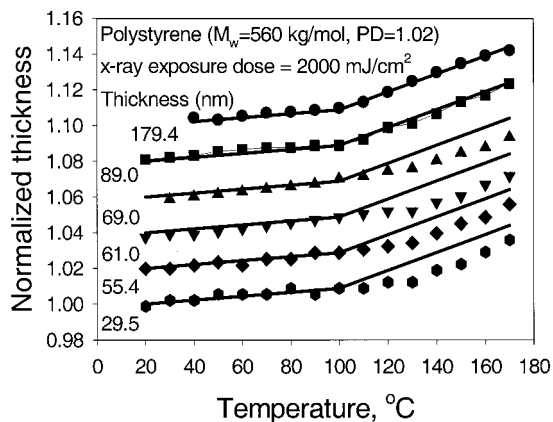

Figure 6. Thickness calculated from the best fit model electron density structure to the X-ray reflectivity data for PS (a) and PMMA (b). The solid points have been obtained with decreasing temperature increments and the hollow symbols with increasing temperature increments. The solid lines are the predictions for the CTE including a correction for Poisson's ratio based on the bulk behavior of the polymer.

resulted in a larger deviation from the predicted thermal expansion behavior of the polymer, specifically, the bulk glass transition temperature. The observed trends in the behavior are similar to what was observed for the same exposure dose values using local thermal analysis and ellipsometry. The precise temperature corresponding to the crossover from glassy to rubbery behavior in the film is difficult to determine since the data was taken in 10 °C temperature increments.

Figure 7 is a plot of the increase in PS film thickness, on OTS surfaces exposed with X-rays at a dose of 2000 mJ/cm², as a function of temperature measured with X-ray reflectivity on five films ranging from 30 to 182 nm thick. All film thickness data were normalized to the value of thickness at 20 °C. The data represent the thickness measured with decreasing temperature increments from 170 to 20 °C. As in the previous plots, the solid lines represent the predicted value of film expansion with temperature assuming bulk properties (coefficient of thermal expansion, Poisson ratio, and glass transition temperature). For films on a surface with 2000 mJ/cm² exposure, consistently larger values of T_g with decreasing film thickness were observed without significant difference in the CTE of the glassy or rubbery regime between the film and the bulk.

Comparison of Techniques to Determine T_g and CTE. Ellipsometry, XRR, and local thermal analysis are well-established techniques for measuring the properties of ultrathin films. This first of a kind side-by-side comparison of results on the same samples highlights the strengths and weaknesses of the techniques. Using

Figure 7. Normalized thickness calculated from the best fit model electron density structure to the X-ray reflectivity data for a PS film supported on OTS exposed to X-rays at a dose of 2000 mJ/cm². Dividing the thickness at one temperature by the thickness at the lowest temperature measured was used to normalize the thickness value. The solid lines are the predictions for the CTE including a correction for Poisson's ratio based on the bulk behavior of the polymer.

ellipsometry and XRR, T_g is determined by measuring changes in the thermal expansion of the film. In ellipsometry, the thickness of the film is determined at each temperature from measurement of the reflection of three wavelengths at a fixed angle. Data can be gathered with relative ease for a large number of points over the temperature range of interest, and the change in slope indicative of T_g is easily detected. The CTE determined by ellipsometry, however, rarely if ever matches the bulk values, even though the ratio of the measured glassy CTE to rubbery CTE is consistent with the ratio of the bulk values. For XRR, the thickness of the film at each temperature is determined from fitting the reflected intensity of a single wavelength over an angular range to an electron density model. It is experimentally impractical to make a large number of thickness measurements using XRR, so the temperature resolution of the XRR experiments is poorer than that of the ellipsometry experiments. Using XRR, it is difficult to obtain a precise T_g value. The CTE values determined by XRR, however, are in good agreement with the bulk values both below and above T_g. Using local thermal analysis, on the other hand, T_g is determined by measuring changes in the heat capacity and thermal conductivity of the film and the area of contact between the probe and the polymer surface. Local thermal analysis is extremely useful for determining T_g, but yields no information on the CTE.

Conclusions

The glass transition temperatures of ultrathin films of polystyrene and poly(methyl methacrylate) depend strongly on thickness and the interfacial energy between the polymer film and the substrate. At low values of the interfacial energy, the T_g of the polymer films was less than the corresponding bulk value. At high values of the interfacial energy, the T_g of the polymer films was greater than the corresponding bulk value. The deviations of the T_g's of the films from the T_g's of the bulk polymers increased with decreasing film thickness. For 20 nm thick films of PS and PMMA, the T_g increased linearly with interfacial energy at 7 °C/(mJ/m²). The glass transition temperatures on the films were determined using both micro-heat-transfer measurements

(local thermal analysis) and thermal expansion measurements (ellipsometry and X-ray reflectivity) and yielded quantitatively consistent results.

References and Notes

(1) Frank, C. W.; Rao, V.; Despotopoulou, M. M.; Pease, R. F. W.; Hinsberg, W. D.; Miller, R. D.; Rabolt, J. F. *Science* **1996**, *273*, 912.
(2) Frank, B.; Gast, A. P.; Russell, T. P.; Brown, H. R.; Hawker, C. *Macromolecules* **1996**, *29*, 6531.
(3) Hall, D. B.; Torkelson, J. M. *Macromolecules* **1998**, *31*, 8817.
(4) Reiter, G.; Sharma, A.; Khanna, R.; Casoli, A.; David, M. O. *J. Colloid Interface Sci.* **1999**, *214*, 126.
(5) Forrest, J. A.; Svanberg, C.; Revesz, K.; Rodahl, M.; Torell, L. M.; Kasemo, B. *Phys. Rev. E* **1998**, *58*, R1226.
(6) Zheng, X.; Rafailovich, M. H.; Sokolov, J.; Strzhemechny, Y.; Schwarz, S. A.; Sauer, B. B.; Rubinstein, M. *Phys. Rev. Lett.* **1997**, *79*, 241.
(7) Forrest, J. A.; DalnokiVeress, K.; Dutcher, J. R. *Phys. Rev. E* **1997**, *56*, 5705.
(8) Forrest, J. A.; Mattsson, J. *Phys. Rev. E* **2000**, *61*, R53.
(9) Fryer, D. S.; Nealey, P. F.; de Pablo, J. J. *Macromolecules* **2000**, *33*, 3376.
(10) Fukao, K.; Miyamoto, Y. *Phys. Rev. E* **2000**, *61*, 1743.
(11) Gidley, D. W.; DeMaggio, G. B.; Frieze, W. E.; Zhu, M.; Hristov, H. A.; Yee, A. F. *Positron Annihilation* **1997**, *255–2*, 635.
(12) Grohens, Y.; Brogly, M.; Labbe, C.; David, M. O.; Schultz, J. *Langmuir* **1998**, *14*, 2929.
(13) Keddie, J. L.; Jones, R. A. L.; Cory, R. A. *Faraday Discuss.* **1994**, 219.
(14) Keddie, J. L.; Jones, R. A. L.; Cory, R. A. *Europhys. Lett.* **1994**, *27*, 59.
(15) vanZanten, J. H.; Wallace, W. E.; Wu, W. L. *Phys. Rev. E* **1996**, *53*, R2053.
(16) Wallace, W. E.; Vanzanten, J. H.; Wu, W. L. *Phys. Rev. E* **1995**, *52*, R3329.
(17) Kim, J. H.; Jang, J.; Zin, W. C. *Langmuir* **2000**, *16*, 4064.
(18) Baschnagel, J.; Binder, K. *Macromolecules* **1995**, *28*, 6808.
(19) Torres, J. A.; Nealey, P. F.; de Pablo, J. J. *Phys. Rev. Lett.* **2000**, *85*, 3221.
(20) Peters, R. D.; Yang, X. M.; Kim, T. K.; Sohn, B. H.; Nealey, P. F. *Langmuir* **2000**, *16*, 4625.
(21) Identification of a commercial product is made only to facilitate experimental reproducibility and to describe adequately experimental procedure. In no case does it imply endorsement by NIST or imply that it is necessarily the best product for the experiment.
(22) Pylkki, R. J.; Moyer, P. J.; West, P. E. *Jpn. J. Appl. Phys., Part 1* **1994**, *33*, 3785.
(23) Russell, T. P. *Mater. Sci. Rep.* **1990**, *5*, 171.
(24) Kim, T. K.; Yang, X. M.; Peters, R. D.; Sohn, B. H.; Nealey, P. F. *J. Phys. Chem. B* **2000**, *104*, 7403.
(25) Lee, L. H. *Langmuir* **1996**, *12*, 1681.
(26) Good, R. J.; Girifalco, L. A. *J. Phys. Chem.* **1960**, *64*, 561.
(27) van Oss, C. J.; Chaudhury, M. K.; Good, R. J. *Chem. Rev.* **1988**, *88*, 927.
(28) Wu, S. *J. Phys. Chem.* **1970**, *74*, 632.
(29) Kahle, O.; Wielsch, U.; Metzner, H.; Bauer, J.; Uhlig, C.; Zawatzki, C. *Thin Solid Films* **1998**, *313*, 803.
(30) Burns, A. R.; Houston, J. E.; Carpick, R. W.; Michalske, T. A. *Langmuir* **1999**, *15*, 2922.
(31) Rowlinson, J. S.; Widom, B. *Molecular Theory of Capillarity*; Clarendon: Oxford, 1982.
(32) Ediger, M. D. *Annu. Rev. Phys. Chem.* **2000**, *51*, 99.

MA001932Q